Bioorganic & Medicinal Chemistry Letters 20 (2010) 5147–5152

Contents lists available at ScienceDirect

Bioorganic & Medicinal Chemistry Letters

journal homepage: www.elsevier.com/locate/bmcl

Discovery and expanded SAR of 4,4-disubstituted quinazolin-2-ones as potent T-type calcium channel antagonists

Kelly-Ann S. Schlegel [a,*], Zhi-Qiang Yang [a], Thomas S. Reger [a], Youheng Shu [a], Rowena Cube [a], Kenneth E. Rittle [a], Phung Bondiskey [a], Mark G. Bock [a], George D. Hartman [a], Cuyue Tang [b], Jeanine Ballard [b], Yuhsin Kuo [b], Thomayant Prueksaritanont [b], Cindy E. Nuss [c], Scott M. Doran [c], Steven V. Fox [c], Susan L. Garson [c], Richard L. Kraus [c], Yuxing Li [c], Victor N. Uebele [c], John J. Renger [c], James C. Barrow [a]

[a] Department of Medicinal Chemistry, Merck & Co., Inc., 770 Sumneytown Pike, P.O. Box 4, West Point, PA 19486, USA
[b] Department of Drug Metabolism and Pharmacokinetics, Merck & Co., Inc., 770 Sumneytown Pike, P.O. Box 4, West Point, PA 19486, USA
[c] Department of Depression and Circadian Disorders, Merck & Co., Inc., 770 Sumneytown Pike, P.O. Box 4, West Point, PA 19486, USA

ARTICLE INFO

Article history:
Received 11 May 2010
Revised 2 July 2010
Accepted 6 July 2010
Available online 8 July 2010

Keywords:
Quinazolin-2-ones
Calcium channel antagonists
T-Type calcium channel
Epilepsy

ABSTRACT

The discovery and synthesis of 4,4-disubstituted quinazolinones as T-type calcium channel antagonists is reported. Based on lead compounds **2** and **3**, a focused SAR campaign driven by the optimization of potency, metabolic stability, and pharmacokinetic profile identified **45** as a potent T-type Ca^{2+} channel antagonist with minimized PXR activation. In vivo, **45** suppressed seizure frequency in a rat model of absence epilepsy and showed significant alterations of sleep architecture after oral dosing to rats as measured by EEG.

Voltage-gated calcium channels play an important role in many physiological processes.[1,2] The Cav3.x family or T-type calcium channels are one class of voltage-gated calcium channels being targeted for the treatment of peripheral and central nervous system (CNS) disorders. T-Type Ca^{2+} channels are classified into three categories: Cav3.1 (α1G), Cav3.2 (α1H), and Cav3.3 (α1I). The α1G and α1I subunits are expressed primarily in the brain, while the α1H subunit has a broader and more peripheral expression.[3] The vast distribution of the T-type Ca^{2+} channels makes them a potential target for the treatment of a number of CNS disorders including sleep,[4,5] epilepsy,[6] schizophrenia,[7] and pain.[8] In the brain, T-type Ca^{2+} channels are highly expressed in the cortex and thalamus, where they play an important role in the proper functioning of thalamocortical signalling.[9,10]

In the late 1990s, mibefradil was identified as the first T-type Ca^{2+} channel antagonist for the treatment of hypertension.[11] Although it is reported to be selective for the T-type channels,[12,13] the outcomes of additional in vivo studies suggested reason for caution when interpreting its effects.[14] Despite these findings, mibefradil is still used as the prototypical T-type antagonist. Earlier reports from our laboratories identified a series of piperidine-derived, selective T-type calcium channel antagonists that demonstrated in vivo efficacy in epilepsy and tremor models without significant cardiovascular effects.[15,16] We sought to identify a novel series of selective T-type Ca^{2+} channel antagonists and demonstrate their in vitro and in vivo activity for the treatment of CNS disorders.

Recently we reported a novel class of potent and selective T-type calcium channel antagonists identified via an HTS campaign based on the quinazolinone core as shown in Figure 1.[17] This class of quinazolinones was originally prepared as non-nucleoside reverse transcriptase inhibitors (NNRTI). Since this core has been extensively studied, its chemical and physical properties were relatively well known, making it an attractive lead.[18] The in vitro potency of compound **1** as shown in Figure 1 was determined via two primary screening assays, the hyperpolarized and depolarized FLIPR assay.[19] Optimization of **1** led to the identification of quinazolinones **2** and **3** as previously disclosed.[17] Herein, we expand on the SAR and discuss the in vivo and in vitro profiles of additional compounds in this series.

We determined that the trifluoroethyl group was optimal at the 3-position based on its potency and metabolically robust nature.[17,18] This knowledge allowed for a focused SAR campaign of the 4-position. Various 6-chloro, 4,4-disubstituted quinazolinones, where R^1 and R^2 are alkyl or aryl, were prepared via previously reported methods[17,18] as shown in Scheme 1. Utilizing a hydroxyl or halogen handle, modification of the aryl substituent was

* Corresponding author. Tel.: +1 215 652 2888; fax: +1 215 652 3971.
E-mail address: kelly_ann_bieber@merck.com (K.-A. S. Schlegel).

0960-894X/$ - see front matter © 2010 Elsevier Ltd. All rights reserved.
doi:10.1016/j.bmcl.2010.07.010

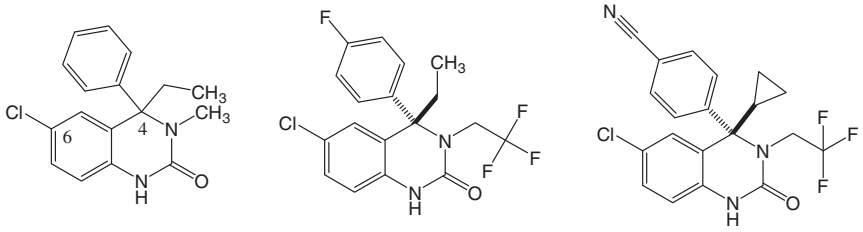

	1	2 (TTA-Q5)	3 (TTA-Q6)
α1i FLIPR IP Hyperpolarized	2172 nM	239 nM	590 nM
α1i FLIPR IP Depolarized	847 nM	61 nM	14 nM

Figure 1. T-Type calcium channel antagonists.

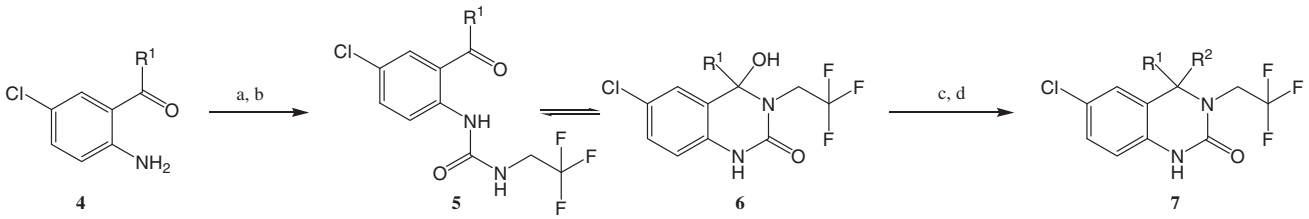

Scheme 1. Reagents and conditions: (a) CDI, CH_2Cl_2, 45 °C; (b) $NH_2CH_2CF_3$, THF, 50 °C; (c) Et_3N, $SOCl_2$, THF, −5 °C; (d) R^2MgBr, THF, −5 °C.

performed via cross-coupling or displacement chemistry as shown in Scheme 2.

Incorporation of fluorine atoms on the alkyl substituent is shown in Scheme 3. The addition of allyl magnesium bromide leads to the formation of quinazolinone **10**. Subsequent ozonolysis provides aldehyde **11** which can be directly treated with DAST to produce compound **12**. Alternatively, **11** can be reduced to the primary alcohol and then treated with DAST to yield compound **13.**

A variety of halogen substitution patterns on the quinazolinone core were explored, and some of these compounds can be prepared via synthetic methods analogous to those reported for NNRTI[18] and TTA-Q5 and Q6.[17] However, when fluorine atoms were incorporated at both the 5- and 6-positions, it was not possible to prepare 4,4-disubstituted quinazolinones as previously reported. Alternate conditions are given in Scheme 4. The amino benzophenone **14** was treated with base and triphosgene followed by the addition of 2,2,2-trifluoroethyl amine producing a mixture of **15** and **16**. Unlike previous reports,[17] the mixture did not proceed directly to product **17** via the procedure of Magnus et al.[20] In this series, the mixture was refluxed in THF in the presence of triethylamine. The reaction mixture was then cooled to −78 °C, and thionyl chloride was added, followed by the appropriate Grignard reagent to afford the 5,6-difluoro, 4,4-disubstituted quinazolinone **17**.[21]

Quinazolinones were screened for potency via depolarized and hyperpolarized FLIPR assays as previously described.[19] Because of the state-dependent nature of these quinazolinone-type inhibitors,[17] the depolarized FLIPR assay became the primary screening assay as this assay proved to be the best overall predictor of in vivo activity. Structure–activity relationships for the 4-position are shown in Table 1 (compounds **18**–**25**). It is important to note that the synthetic route provides racemic quinazolinones. Racemates showing activity in the FLIPR assay were subjected to resolution by chiral HPLC, and the enantiomers were tested individually. As demonstrated by **18** and **19**, when both R^4 and

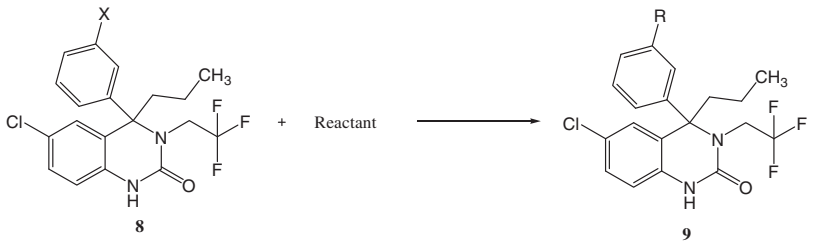

Scheme 2. Reagents and conditions:

X	Reactant	R	Catalyst	Base	Solvent	Temp (°C)	Time (min)
O	2-Fluoropyridine	O-2-Pyr	—	Cs_2CO_3	—	130	30
Br	Ar–$B(OH)_2$	Ar	$P(Cy)_3$, Pd_2dba_3	K_3PO_4	Dioxane	150	30
Br	Ar–$Sn(Bu)_3$	Ar	$Pd(PPh_3)_4$	—	Dioxane	150	30
Br	Morpholine	Morpholine	CuI, proline	K_2CO_3	DMSO	150	30

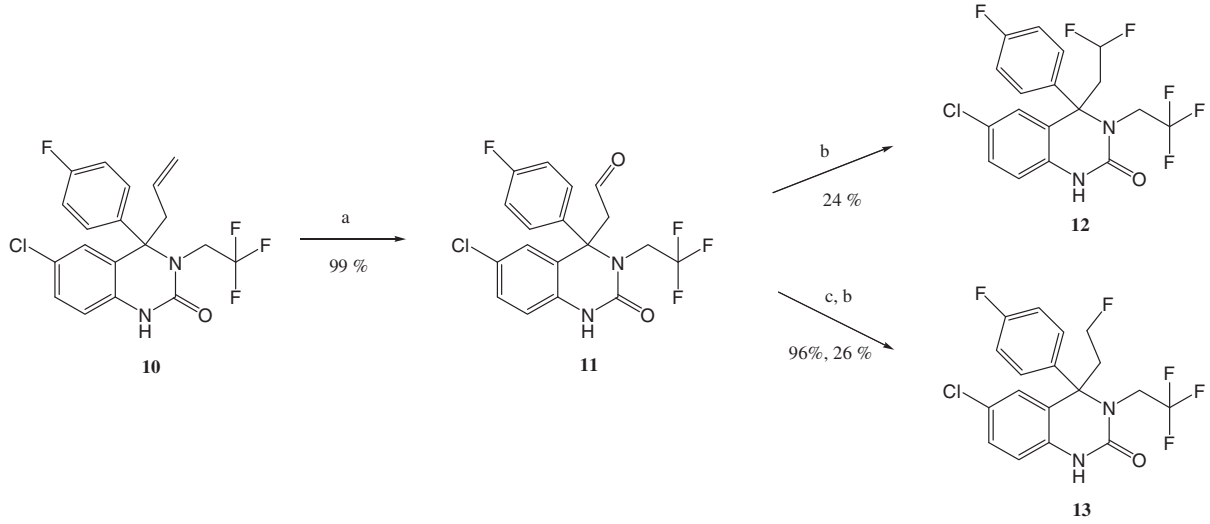

Scheme 3. Reagents and conditions: (a) (1) ozone, MeOH, −78 °C; (2) dimethyl sulfide, −78 °C to rt; (b) DAST, 0 °C, CH_2Cl_2; (c) $NaBH_4$, MeOH, 0 °C to rt.

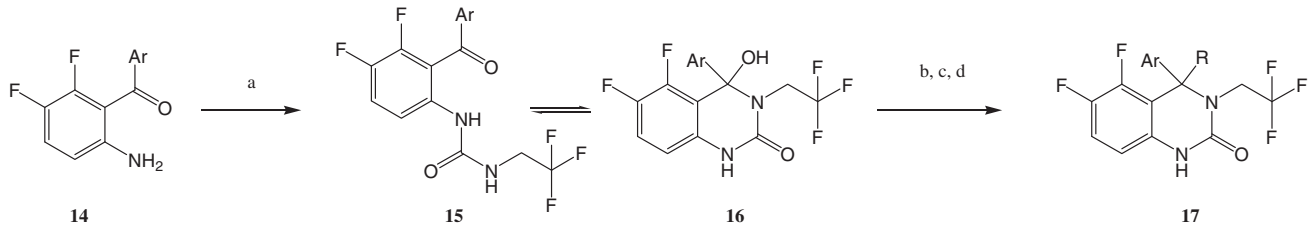

Scheme 4. Reagents and conditions: (a) triphosgene, Et_3N, $CF_3CH_2NH_2$, ether, 0 °C to rt; (b) Et_3N, THF, 80 °C, 1 h; (c) $SOCl_2$, THF, −78 °C; (d) RMgBr, THF, −78 °C.

$R^{4'}$ are alkyl, lower activity in the FLIPR assay is observed. Enhanced potency is achieved when R^4 = aryl and $R^{4'}$ = a small alkyl group as exemplified in **21A**. Compounds **21A** and **21B** are single enantiomers with a >50-fold difference in FLIPR activity, which is typical for quinazolinone isomers. Absolute configurations were not determined, but the active isomer is assumed to be similar to **2** and **3** which were previously established.[17]

SAR of the aryl substituent was further explored via the incorporation of substituents in the 3- and 4-positions as shown in Table 1 (examples **22** through **29**). Incorporation of a methoxy substituent in the 3- or 4-position was not well tolerated. The 4-fluorophenyl group provided the best activity as measured by the FLIPR assay where the active enantiomer **24A** demonstrated a potency of 25 nM. The 3,4-difluorophenyl substituent in **25** shows decreased potency. Further SAR of the 3-position was explored via the incorporation of heterocycles as shown in examples **26** through **29**. These heterocyclic derivatives exhibited potency in the FLIPR assay and enhanced physical properties due to their increased polarity.

A small alkyl substituent such as ethyl, propyl, or cyclopropyl as one of the groups at the quinazolinone 4-position yields optimal FLIPR potency; however, these alkyl groups were identified as a metabolic liability. To block a potential metabolic site, fluoroalkanes **30A, 30B, 31A** and **31B** were prepared. While **30A** and **31A** show reasonable potency in our FLIPR assay, they did not significantly improve the potency of TTA-Q5 (61 nM).

While TTA-Q5 (**2**) showed good potency, selectivity, and vivo efficacy,[17] it was a pregnane X receptor (PXR) activator as were many compounds in the 6-chloro quinazolinone series. TTA-Q5 showed PXR activation of 63% compared to the positive control Rifampicin at 10 μM. PXR is a potential liability as it could lead to CYP3A4 activation; therefore, causing undesirable drug–drug interactions.[22,23] As a way to mitigate PXR activation, the halogen substituent and substitution pattern on the quinazolinone core were explored as shown in Table 2. Incorporation of a fluorine atom at the 5-position in conjunction with the 6-chloro substituent (compound **32**) showed a decrease in FLIPR potency. Removal of the 6-chloro substituent coupled with the incorporation of a 5-fluoro (**33**) or 5,8-difluoro (**34**) substituent showed a decrease in FLIPR potency and an increase in PXR activation. Replacement of the 6-chloro substituent with a fluorine atom as in **35A** provided comparable FLIPR potency and PXR activation with TTA-Q5. In contrast, its enantiomer **35B** showed decreased FLIPR potency. A 5,6-difluoro substituent as in **36A** maintained good FLIPR potency and showed a decreased propensity for PXR activation when compared to TTA-Q5. The 6-fluoro and 5,6-difluoro substitution patterns exemplified by **35A** and **36A** were chosen for further SAR studies.

In the 6-chloro quinazolinone series, FLIPR potency was greatly dependent upon the composition of the 4-aryl and 4-alkyl substituents. This trend is also observed in the 6-fluoro and 5,6-difluoro quinazolinone series as shown in Table 3. Introduction of the *n*-propyl group as in **37** provides a boost in FLIPR potency. Incorporation of a bulky *t*-butyl group in **38** or a polar group in **42** and **43** as the 4-alkyl substituent is not well tolerated and caused a decrease in FLIPR potency. The previously identified 4-fluorophenyl and ethyl substituents employed in TTA-Q5 provided an increase in FLIPR potency and a modest reduction of PXR activation in both our 6-fluoro and 5,6-difluoro quinazolinone series (**39** and **40**). A slightly longer alkyl chain (*n*-propyl) as in **41** also provided an increase in FLIPR potency.

Metabolic stability became an issue with the 6-fluoro and 5,6-difluoro quinazolinone series. When **40** was incubated with human liver microsomes, less than 1% of compound remained after

Table 1
SAR of the 4-position

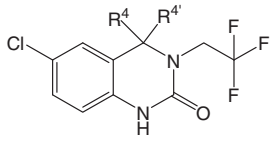

Example	R^4	$R^{4'}$	α1I FLIPR IP depolarized (nM)[a]
18	Cyclopropyl	*n*-Butyl	111 ± 30
19	Cyclopropyl	*sec*-Butyl	447 ± 66
20	Phenyl	Allyl	87 ± 12
21A	Phenyl	Ethyl	71 ± 29
21B	Phenyl	Ethyl	3885 ± 1024
22	4-Methoxy phenyl	*n*-Propyl	879 ± 438
23	3-Methoxy phenyl	*n*-Propyl	171 ± 54
24A	4-Fluorophenyl	*n*-Propyl	25 ± 11
24B	4-Fluorophenyl	*n*-Propyl	1317
25	3,4-Difluorophenyl	Ethyl	141 ± 43
26	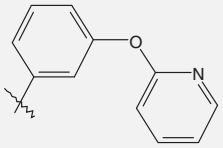	*n*-Propyl	73 ± 33
27	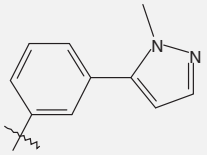	*n*-propyl	318 ± 119
28	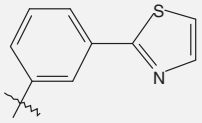	*n*-Propyl	62 ± 29
29	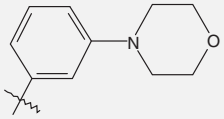	*n*-Propyl	161 ± 60
30A	4-Fluorophenyl	CH_2CH_2F	42 ± 15
30B	4-Fluorophenyl	CH_2CH_2F	905[b]
31A	4-Fluorophenyl	CH_2CHF_2	60 ± 12
31B	4-Fluorophenyl	CH_2CHF_2	469[b]

[a] All values are the mean ± the standard deviation of at least *n* = 3 measurements. Assay described in Ref. 19.
[b] Indicates single data point.

60 min.[25] The ethyl chain was identified as the primary metabolic site. To block metabolism, the fluoroalkanes employed in the 6-chloroquinazolinone series were prepared. The monofluoroethyl derivative (**44**, a single enantiomer) improved potency, maintained lower propensity for PXR activation, and improved stability in human liver microsomes (66 ± 2% remaining at 60 min). When a difluoroethyl group is installed at the 4-position (**45**, a single enantiomer[26]), potency is improved to 14 nM, PXR activation is reduced (35%), and metabolic stability is improved (68 ± 9% at 60 min). The FLIPR potency was confirmed by whole cell patch clamp recording at two holding potentials, −100 mV and −80 mV, and **45** showed potencies of 190 nM and 31 nM, respectively.

The pharmacokinetic profile of **45** is shown in Table 5. Compound **45** shows a reasonable pharmacokinetic profile across three species, with $t_{1/2}$ between 1 and 6 h, but exhibits modest bioavailability in rat and monkey. Compound **45** is not an inhibitor of any major CYPs, nor is it a time-dependent inhibitor of CYP3A4. It is not a P-gp substrate in human (BA/AB ratio = 1.2) or rat (BA/AB ratio = 1.5).[27] The plasma protein binding was determined to be 98.5% in human and 97.9% in rat.

Table 2
SAR of 5-,6- and 8-positions

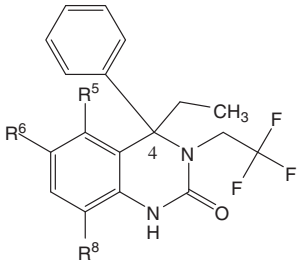

Example	R^5	R^6	R^8	α1I FLIPR IP depolarized (nM)[a]	PXR (% Rif at 10 μM)[b]
32	F	Cl	H	132 ± 38	61
33	F	H	H	111 ± 17	83
34	F	H	F	657 ± 294	91
35A	H	F	H	50 ± 29	63
35B	H	F	H	3739[c]	74
36A	F	F	H	20 ± 2	48
36B	F	F	H	2039[c]	ND[d]

[a] All values are the mean ± the standard deviation of at least *n* = 3 measurements. Assay described in Ref. 19.
[b] See Ref. 24.
[c] Indicates single data point.
[d] Not determined.

Table 3
4-Position SAR of 6-fluoro and 5,6-difluoro quinazolinones

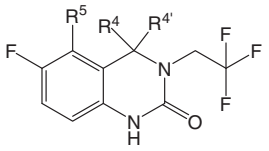

Example	R^4	$R^{4'}$	R^5	α1I FLIPR IP depolarized (nM)[a]	PXR (% Rif at 10 μM)[b]
37	Phenyl	*n*-Propyl	H	38 ± 24	49
38	Phenyl	*t*-Butyl	H	757 ± 376	44
39[c]	4-Fluorophenyl	Ethyl	H	25 ± 13	58
40[c]	4-Fluorophenyl	Ethyl	F	16 ± 6	52
41[c]	4-Fluorophenyl	*n*-Propyl	F	9 ± 4	73
42	4-Fluorophenyl	Nitrile	F	290 ± 46	ND[d]
43	4-Fluorophenyl	CH_2CH_2OH	F	3089 ± 284	ND[d]
44[c]	4-Fluorophenyl	CH_2CH_2F	F	17 ± 4	53
45[c]	4-Fluorophenyl	CH_2CHF_2	F	14 ± 8	35

[a] All values are the mean ± the standard deviation of at least *n* = 3 measurements. Assay described in reference 19.
[b] See Ref. 24.
[c] Indicates active enantiomer.
[d] ND = not determined.

To further probe the SAR of the quinazolinone series, substitution at the 1-position of the quinazolinone core was explored. Compounds were prepared by treatment of the quinazolinone core with base followed by the addition of an alkyl halide or acid chloride. A representative subset of these compounds is shown in Table 4. Many structural changes are not tolerated and result in a decrease in potency as in **47** and **48** or an increase in PXR activation as in **46**. The incorporation of the methyl 4-pyridyl N-oxide moiety maintained potency while decreasing PXR activation as in examples **49** and **50**; however, these two compounds showed poor metabolic stability in human liver microsomes with only 3.8 ± 1% and 18 ± 3% remaining after 30 min, respectively. Incorporation of a monofluoroethyl substituent at the 4-position in combination with the methyl 4-pyridyl N-oxide substituent in the 1-position (**51**) produced a potent (38 nM) compound with reasonable metabolic

Table 4
1-Position SAR of 5,6-difluoro-4,4-disubstituted quinazolinones

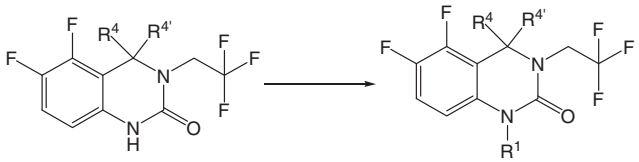

Example	R^4	$R^{4'}$	R^1	α1I FLIPR IP depolarized (nM)[a]	PXR (% Rif at 10 μM)[b]
46[c]	4-Fluorophenyl	Ethyl	$CH_2CH_2OCH_3$	53 ± 26	70
47[c]	4-Fluorophenyl	Ethyl	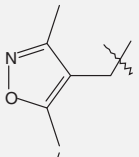	1833 ± 460	ND[d]
48[c]	4-Fluorophenyl	Ethyl	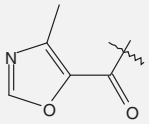	127 ± 12	ND[d]
49[c]	4-Fluorophenyl	Ethyl	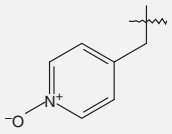	12 ± 4	26
50[c]	4-Fluorophenyl	*n*-Propyl	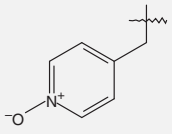	6 ± 1	11
51[c]	4-Fluorophenyl	CH_2CH_2F	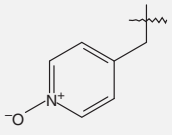	38 ± 5	56

[a] All values are the mean ± the standard deviation of at least $n = 3$ measurements. Assay described in Ref. 19.
[b] See Ref. 24.
[c] Indicates active enantiomer.
[d] ND = not determined.

Table 5
Pharmacokinetic profiles

Species	CL_p (mL/min/kg)	$t_{1/2}$ (h)	Vd_{ss} (L/kg)	*F* (%)
Pharmacokinetic profile of ***45***				
Rat	55	1.6	6.7	15
Dog	10.5	5.9	3.6	
Monkey	23	5.8	9.8	15
Pharmacokinetic profile of ***49***				
Rat	21	1.1	1.7	22
Dog	3.5	1.3	0.37	

stability (59 ± 3% remaining after 60 min); however, it became a PXR activator.

Compound **49** (single, active enantiomer**)** was more fully profiled and showed moderate clearance and short half-life in rat and dog as shown in Table 5. Although **49** had lower plasma protein binding (89% bound), it was a P-gp substrate in rat (BA/AB ratio = 7).

On the strength of its potency, relative metabolic stability, and reduced PXR activation, the efficacy of compound **45** was evaluated in our primary in vivo screening model of absence epilepsy. This model uses Wistar Albino Glaxo rats bred in Rijswijk, The Netherlands (WAG/Rij), which display EEG patterns and behaviors typical of epileptic conditions, including excessive seizures.[28] Because of the involvement of T-type Ca^{2+} channels in the thalamocortical network that is believed to play a role in these seizures, EEG measurement of seizure suppression in WAG/Rij rats can be interpreted as T-type Ca^{2+} channel inhibition. A 3 mg/kg oral dose of **45** to WAG/Rij rats resulted in a 44% inhibition of total seizure time at 4 hours post dose. An inhibition of 70% is observed with a 10 mg/kg oral dose of **45** at 4 h post dose.

To evaluate the effects of a T-type calcium channel antagonist on vigilance, **45** was dosed in a seven day crossover rat study. In this study, electrocorticogram (ECoG) and electromyogram (EMG) signals were measured in rats and scored for the time spent awake, in light sleep, delta sleep, or REM. The rats received a 10 mg/kg oral dose of **45** 30 min prior to their inactive (sleep) phase. As shown in Figure 2, a decrease in active wake and REM and an increase in delta sleep are observed immediately post dose. These effects persisted for up to 3 h. During this study an exposure of 6 μM·h was reached, resulting in the observed robust effect on sleep architecture. The effect of other selective T-type Ca^{2+} channel antagonists such as TTA-Q6 and other quinazolinones,[17] piperidine-derived analogs,[15,16] and TTA-A2[29] on rat sleep have been previously reported. All show results similar to those observed for **45** providing further evidence for the involvement of T-type calcium channels in vigilance state maintenance.

In conclusion, the SAR of the quinazolinone series was explored and optimized on the basis of T-type Ca^{2+} channel potency, PXR

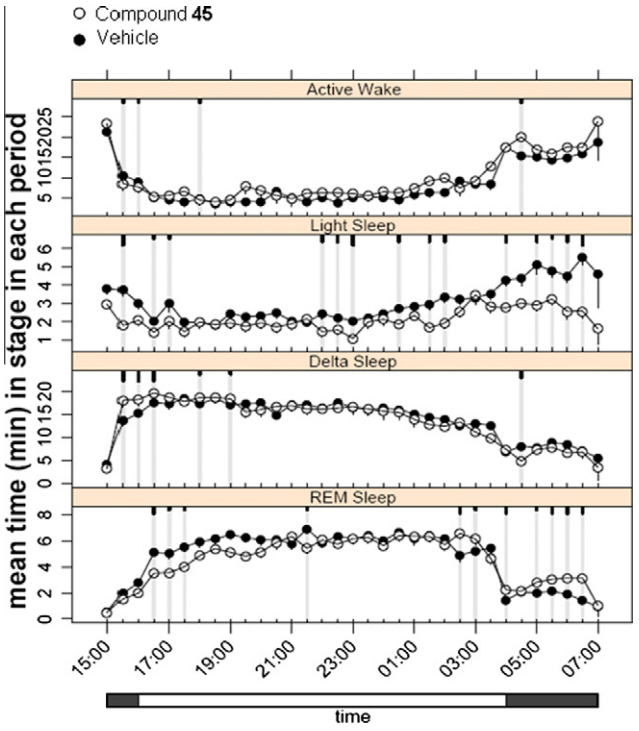

Figure 2. Effect of **45** (single, active enantiomer) on $n = 7$ male rat for active, light, delta, and REM sleep for 16 h after dosing 10 mg/kg PO. Data is average minutes of active wake, light sleep, delta sleep, or REM in each 30 min bins (±SEM) starting at dose time (abscissa 15:00). Significance at each time point reported as tick marks (short = p <0.05, medium = p <0.01, long = p <0.001) and gray vertical lines through significantly different comparisons based on a linear mixed effects ANOVA at each time point.

activation, metabolic stability and pharmacokinetic profile. The tractable SAR of the quinazolinone series led to the discovery of potent T-type Ca^{2+} channel antagonist **45**, which suppressed seizure activity in the WAG/Rij model and altered the sleep architecture of rats. These findings suggest that T-type Ca^{2+} channel antagonists could potentially be used for the treatment of a number of CNS disorders.

Acknowledgments

The authors thank Nicole Pudvah for PGP measurements, Ken Anderson, Leslie Geer, and Debra McLoughlin for PK analysis, Charles Ross and Joan Murphy for high resolution mass spectral analysis, and Carl Homnick, ZhiQiang Wang, and Todd Anderson for chiral separations.

References and notes

1. Zamponi, G. W. *Voltage-Gated Calcium Channels*; Kluwer Academic/Plenum, 2005.
2. Tsien, R. W.; Wheeler, D. B. In *Calcium as a Cellular Regulator*; Carafoli, E., Klee, C., Eds.; Oxford University Press: New York, 1999; pp 171–199.
3. Talley, E. M.; Cribbs, L. L.; Lee, J. H.; Daud, A.; Perez-Reyes, E.; Bayliss, D. *J. Neurosci.* **1999**, *19*, 1895.
4. Llinas, R. R.; Steriade, M. *J. Neurophysiol.* **2006**, *95*, 3297.
5. Crunelli, V.; Cope, D. W.; Hughes, S. W. *Cell Calcium* **2006**, *40*, 175.
6. Varela, D.; Khosravani, H.; Heron, S. E.; Bladen, C.; Williams, T. C.; Newman, M.; Berkovic, S. F.; Scheffer, I. E.; Mulley, J. C.; Zamponi, G. W. Biophysical Society Meeting Abstracts. *Biophys. J.* **2007**, 2868.
7. Zhang, Y.; Llinas, R. R.; Lisman, J. E. *Front Neural Circuits* **2009**, *3*, 20.
8. Todorovic, S. M.; Jevtovic-Todorovic, V. *CNS Neurol. Disord.: Drug Targets* **2006**, *5*, 639.
9. Cueni, L.; Canepari, M.; Adelman, J. P.; Luthi, A. *Pflug. Arch. Eur. J. Phy.* **2009**, *457*, 1161.
10. Bessaih, T.; Leresche, N.; Lambert, R. C. *Proc. Natl Acad. Sci. U.S.A.* **2008**, *105*, 11376.
11. Clozel, J. P.; Ertel, E. A.; Ertel, S. I. *J. Hypertens.* **1997**, *15*, S17.
12. Mehrke, G.; Flockerzi, V.; Hofmann, F. *J. Pharmacol. Exp. Ther.* **1994**, *271*, 1483.
13. Bezprozvanny, I.; Tsien, R. W. *Mol. Pharmacol.* **1995**, *48*, 540.
14. Moosmang, S.; Haider, N.; Bruderl, B.; Welling, A.; Hofmann, F. *Circ. Res.* **2006**, *98*, 105.
15. Shipe, W. D.; Barrow, J. C.; Yang, Z.-Q.; Lindsley, C. W.; Yang, F. V.; Schlegel, K.-A. S.; Shu, Y.; Rittle, K. E.; Bock, M. G.; Hartman, G. D.; Tang, C.; Ballard, J. E.; Kuo, Y.; Adarayan, E. D.; Prueksaritanont, T.; Zrada, M. M.; Uebele, V. N.; Nuss, C. E.; Connolly, T. M.; Doran, S. M.; Fox, S. V.; Kraus, R. L.; Marino, M. J.; Gratifelds, V. K.; Vargas, H. M.; Bunting, P. B.; Hasbun-Manning, M.; Evans, R. M.; Koblan, K. S.; Renger, J. J. *J. Med. Chem.* **2008**, *51*, 3692.
16. Yang, Z.-Q.; Barrow, J. C.; Shipe, W. D.; Schlegel, K.-A. S.; Shu, Y. S.; Yang, F. V.; Lindsley, C. W.; Rittle, K. E.; Bock, M. G.; Hartman, G. D.; Uebele, V. N.; Nuss, C. E.; Fox, S. V.; Kraus, R. L.; Doran, S. M.; Connolly, T. M.; Tang, C. Y.; Ballard, J. E.; Kuo, Y. S.; Adarayan, E. D.; Prueksaritanont, T.; Zrada, M. M.; Marino, M. J.; Graufelds, V. K.; DiLella, A. G.; Reynolds, I. J.; Vargas, H. M.; Bunting, P. B.; Woltmann, R. F.; Magee, M. M.; Koblan, K. S.; Renger, J. J. *J. Med. Chem.* **2008**, *51*, 6471.
17. Barrow, J. C.; Rittle, K. E.; Reger, T. S.; Yang, Z.-Q.; Bondiskey, P.; McGaughey, G. B.; Bock, M. G.; Hartman, G. D.; Tang, C. Y.; Ballard, J. E.; Kuo, Y. S.; Prueksaritanont, T.; Nuss, C. E.; Doran, S. M.; Fox, S. V.; Garson, S. L.; Kraus, R. L.; Li, Y.; Marino, M. J.; Graufelds, V. K.; Uebele, V. N.; Renger, J. J. *ACS Med. Chem. Lett.* **2010**, *1*, 75.
18. Tucker, T. J.; Lyle, T. A.; Wiscount, C. M.; Britcher, S. F.; Young, S. D.; Sanders, W. M.; Lumma, W. C.; Goldman, M. E.; Obrien, J. A.; Ball, R. G.; Homnick, C. F.; Schleif, W. A.; Emini, E. A.; Huff, J. R.; Anderson, P. S. *J. Med. Chem.* **1994**, *37*, 2437.
19. Uebele, V. N.; Nuss, C. E.; Fox, S. V.; Garson, S. L.; Cristescu, R.; Doran, S. M.; Kraus, R. L.; Santarelli, V. P.; Li, Y.; Barrow, J. C.; Yang, Z. Q.; Schlegel, K. A.; Rittle, K. E.; Reger, T. S.; Bednar, R. A.; Lemaire, W.; Mullen, F. A.; Ballard, J. E.; Tang, C.; Dai, G.; McManus, O. B.; Koblan, K. S.; Renger, J. J. *Cell Biochem. Biophys.* **2009**, *55*, 81.
20. Magnus, N. A.; Confalone, P. N.; Storace, L.; Patel, M.; Wood, C. C.; Davis, W. P.; Parsons, R. L. *J. Org. Chem.* **2003**, *68*, 754.
21. The synthesis of 4,4-disubstituted quinazolinones has been reported in the following patent literature: WO2009009015 and WO2006098969.
22. Sinz, M.; Kim, S.; Zhu, Z.; Chen, T.; Anthony, M.; Dickinson, K.; Rodrigues, A. D. *Curr. Drug Metab.* **2006**, *7*, 375.
23. Based on Ref. 22 and in house data, the following guidelines are used to determine the potential for clinical drug–drug interactions. Using % activation (compared to the positive control Rifampin), the criteria for having a high potential for clinical drug–drug interaction is defined as a value of >40%, between 15% and 40% for moderate potential, and <15% as having a low potential.
24. Gao, Y. D.; Olson, S. H.; Balkovec, J. M.; Zhu, Y.; Royo, I.; Yabut, J.; Evers, R.; Tan, E. Y.; Tang, W.; Hartley, D. P.; Mosley, R. T. *Xenobiotica* **2007**, *37*, 124.
25. For metabolic stability assay, compounds (1 μM) were incubated with human liver microsomes (0.2 mg protein/mL) in the presence of NADPH cofactor for 30 or 60 min at 37 °C.
26. Compound **45** is a single, active enantiomer. All in vitro and in vivo data included for **45** was collected on the active enantiomer.
27. Hochman, J. H.; Pudvah, N.; Qiu, J.; Yamazaki, M.; Tang, C.; Lin, J. H.; Prueksaritanont, T. *Pharm. Res.* **2004**, *21*, 1686–1691.
28. Coenen, A. M. L.; Drinkenburg, W. H. I. M.; Inoue, M.; Vanluijtelaar, E. L. J. M. *Epilepsy Res.* **1992**, *12*, 75.
29. Uebele, V. N.; Gotter, A. L.; Nuss, C. E.; Kraus, R. L.; Doran, S. M.; Garson, S. L.; Reiss, D. R.; Li, Y. X.; Barrow, J. C.; Reger, T. S.; Yang, Z. Q.; Ballard, J. E.; Tang, C. Y.; Metzger, J. M.; Wang, S. P.; Koblan, K. S.; Renger, J. J. *J. Clin. Invest.* **2009**, *119*, 1659.